Macromolecular Research, Vol. 23, No. 9, pp 819-829 (2015)
DOI 10.1007/s13233-015-3109-y

www.springer.com/13233
pISSN 1598-5032 eISSN 2092-7673

Fabrication of Form-Stable Poly(ethylene glycol)-Loaded Poly(vinylidene fluoride) Nanofibers *via* Single and Coaxial Electrospinning

Thu Thi Dang[1], Thuy Thi Thu Nguyen[2], Ok Hee Chung[3], and Jun Seo Park*[,1]

[1]*Department of Chemical Engineering and Research Center of Chemical Technology, Hankyong National University, Gyeonggi 456-749, Korea*
[2]*Faculty of Chemical Technology, Hanoi University of Industry, Hanoi, Vietnam*
[3]*Department of Physics, Sunchon National University, Sunchon, Jeonnam 540-950, Korea*

Received February 12, 2015; Revised June 15, 2015; Accepted June 17, 2015

Abstract: Two types of form-stable phase change material based on poly(ethylene glycol)-loaded poly(vinylidene fluoride) (PVDF) nanofibers were fabricated via single and coaxial electrospinning. Blends of two different kinds of poly(ethylene glycol) (PEG600 and PEG1000) were used as the phase change material (PCM) and PVDF was used as supporting polymers in the PCM-loaded electrospun PVDF nanofibers. By single electrospinning, SiO_2 was added into the PEGs-loaded PVDF to prevent PEGs leakage and to maintain the shape of the nanofibers during the melting and solidifying processes. The addition of SiO_2 also increased the mechanical strength of the nanofibers. By coaxial electrospinning, the core/shell structured nanofibers, in which the PEGs and PVDF were the active core and protective shell layers, respectively, were fabricated. The microstructure of the e-spun nanofibers was investigated by FE-SEM. TEM images show that PEGs were encapsulated by PVDF shell. The ATR-FTIR analysis and water contact angle measurements confirm that good core/shell-structured nanofibers were obtained when the core feed rate was lower than 4.0 μL/min. During the water immersion test, the PEGs on the surface of the PVDF/SiO_2 composite nanofibers were dissolved, while no leakage of PEGs from the core/shell-structured nanofibers was observed. A hot oven and a DSC cycling tests were conducted to evaluate the thermal stability. These results show that the PEGs-loaded core/shell nanofibers had better thermal stability than the PEGs-loaded PVDF/SiO_2 composite nanofibers. Therefore, the non-woven mats of the core/shell-structured nanofibers could have extensive applications in thermal energy storage and fabrication of smart textile.

Keywords: phase change materials, poly(ethylene glycol), electrospinning, form-stability.

Introduction

Phase change materials (PCMs) have been extensively applied in various energy applications owing to their great ability to store or release energy as they change from one physical state to another. PCMs, which include inorganic materials, organic materials, and eutectics, have been studied for several decades in the field of energy research.[1-7] The selection of the PCM for the latent heat thermal energy storage (LHTES) method is very important in order to optimize the thermal efficiency, economic feasibility and utility life of the system.[5,8,9]

Among organic PCMs, poly(ethylene glycol) (PEG) is a functional material for thermal energy storage because of its relatively high latent heat of fusion, congruent melting and freezing behavior, and broad melting temperature range. These properties are dependent on its molecular weight. When PEG materials of different molecular weights are combined, a molecule chain from one PEG material can enter the unit lattice of the other, achieving interpenetration, and thus producing co-crystals.[10,11] The preparation of PEG blends have been investigated by the melt blending method and by dissolution in suitable solvent systems. The resulting form-stable PEG and polymers have subsequently been evaluated.[12] Qian *et al*. reported that the shape-stabilized co-crystallized PEG composites were successfully prepared by the sol-gel process.[10] In his study, the combination of PEG2,000 and PEG10,000 with a suitable ratio (3:1 by weight) led to synergistically increased fusion enthalpy, which was attributed to the co-crystallization effect.

To overcome the leakage of molten PCMs during their application, the form-stable PCMs were prepared by methods such as the self-polymeration method, the sol-gel method, the physical blending method, and electrospinning.[13-20] Among these methods, electrospinning is a simple and versatile technique for the encapsulation of PCM into ultrafine fibers of various polymers.[1,21-26] The nonwoven mats of electrospun (e-spun)

*Corresponding Author. E-mail: jspark@hknu.ac.kr

nanofibers, comprising of PCM and polymers, can be used as effective energy storage materials because of their desirable dimensions, high latent heat values, excellent mechanical strength, and large specific surface areas.[14] Chen *et al.* achieved the fabrication of ultrafine fibers of a PEG/cellulose acetate (CA) composite[1] and a PEG/CA core/sheath structure.[2] In their studies, PEG10,000 and CA were a PCM material and a supporting polymer, respectively. The composite nanofibers had higher latent heat values for melting and crystallization (86.03 and 65.15 J/g, respectively) than those of the core/shell-structured nanofibers (60.8 and 58.7 J/g, respectively). However, Chen did not refer to the thermal stability of the ultrafine fibers. To further improve the thermal stability of the PEG/polymer composite nanofibers, Nguyen *et al*.[14] investigated the preparation of form-stable e-spun nanofibers of PEG1000/SiO_2/PVDF composite nanofibers. The results demonstrated that the addition of SiO_2 to the PVDF/PEG blend helped retain the shape of the fibers, and prevented the leakage of the molten PEG following a heat treatment at 80 ºC for 24 h.

In this study, a PEGs blend of PEG600 and PEG1000 (ratio 1:1 w:w) was prepared as a PCM material. The PEGs blend was used to widen the phase transition temperature in the range of climatic temperature. Therefore, it can be used for many practical applications. Two types of form-stable PCM-loaded poly(vinylidene fluoride) (PVDF) nanofibers (PEGs/PVDF composite nanofibers containing fumed silica and PEGs/PVDF core/shell structured nanofibers) were fabricated by single and coaxial electrospinning, respectively. To prevent the leakage of molten PEGs from the e-spun nanofibers at high temperatures, fumed silica (SiO_2) was added into the PEG/PVDF blend nanofibers. With a similar purpose, PEGs were loaded into the core of the PVDF nanofibers to produce form-stable core/shell nanofibers. The morphology of the PEGs loaded PVDF e-spun nanofibers with various percentages of PEGs and SiO_2 were characterized by field emission scanning electron microscopy (FE-SEM). The structure of the core/shell composite nanofibers were confirmed by water contact angle (WCA) measurement and attenuated total reflectance-Fourier transform infrared (ATR-FTIR), transmission electron microscopy (TEM). In addition, the effect of the SiO_2 component on the tensile properties of the PEG loaded PVDF nanofibers was also evaluated by tensile testing. The evaluation of the form-stability of the blend and core/shell nanofibers was conducted by DSC heating/cooling.

Experimental

Materials. PEGs with average molecular weights (M_w) of 600 and 1,000 Da (g/mol) were supplied by Samchun Co. (Korea). Kynar@761 PVDF was used. *N,N*-Dimethylacetamide (DMAc) and acetone solvents were purchased from Samchun Co. (Korea). Fumed SiO_2 (average particle size: 7 nm) was obtained from Sigma Aldrich. All chemicals were used without further purification.

Electrospinning. The PVDF was dissolved at a concentration of 16 wt% in a mixture of DMAc and acetone (60:40 w/w). The mixture of PEG600 and PEG1000 (PEGs) was obtained by mixing the two types of PEG to a mass ratio of 1:1.

The PEGs blend was mixed with a PVDF solution, using various percentages of PEGs from 0 to 70%. Using these blended solutions, the electrospinning was performed in a single electrospinning apparatus (Nano NC, Korea) at a temperature of 25 ºC. Each prepared solution was poured into a 5 mL plastic syringe (Kovax-Syringe, Korea vaccine Co., Ltd) that was attached to a blunt 22-gauge stainless steel hypodermic needle. A solution flow rate of 1.0 mL/h was controlled using a syringe pump (KD scientific, Model KDS200, U.S.A). The e-spun nanofibers were collected on aluminum foil placed above the flat-grounded metal plate. The applied voltage and the distance between the tip of needle and the collector were maintained at 12 kV and 15 cm, respectively. For the fabrication of PEGs-loaded PVDF/SiO_2 composite nanofibers, fumed silica was added into the polymer solution and the mixed solution was stirred at a temperature of 25 ºC until the mixture became clear.

The coaxial electrospinning was conducted as follows: The 16 wt% PVDF solution was placed in the double spinneret to produce the shell layer. The PEGs blend which was dissolved in ethanol at a concentration of 50 wt%, was the core fluid. The double spinneret consists of a stainless-steel needle with an inner diameter (ID) of 0.35 mm and an outer diameter (OD) of 0.65 mm, while the outer capillary has an ID of 1.05 mm and an OD of 1.20 mm. The solution was placed into 5 mL syringes and fed by a syringe pump (KD scientific, Model KDS200, U.S.A.). Both needles were connected to a high voltage supply. The applied voltage was maintained at 8.5 kV and the distance between the tip of the needles and the collector of 15 cm, respectively. The shell feed rate was set at 2.0 mL/h, while the core feed rate varied from 1.0 to 4.0 μL/min. The electrospinning was performed in air at a temperature of 25 ºC.

Characterizations. The morphology of the non-woven mats of the e-spun nanofibers was examined by FE-SEM (HITACHI S-4700, Japan), using a coating system (BAL-TE MED020). From the FE-SEM photographs, the diameter distributions of e-pun fibers were measured using visualization software (TOMORO ScopeEye 3.6).

The thermal properties of the PCM-loaded e-spun nanofibers (including latent heat and temperature of the melting and crystallization points) were measured by DSC (SH IN2920, TA instrument, USA). The analyses were performed at a heating rate of 5 ºC/min, under a constant stream of nitrogen.

WCA measurements with a video contact angle instrument (Samsung FA-CED camera, Korea) were conducted to detect the leakage of hydrophilic PEGs from the e-spun nanofibers.

The chemical structure of the surface of the core/shell structured coaxial e-spun nanofibers was analyzed by FTIR analysis (JASCO, ATR-FTIR6100, Japan) to detect the leakage of PEGs from the e-spun core/shell (PEGs/PVDF) structured nanofibers.

The mechanical properties of non-woven mats of e-spun nanofibers were characterized using a tensile tester (LR 5K, LLOYD instrument). The nonwoven webs were tested with a 0.1 N preload at a crosshead speed of 5 mm/min.

The core-shell structure of the PCMs was examined using TEM (TecnaiG^2, USA). The samples for TEM were prepared by direct deposition of the e-pun fibers onto copper grids.

Results and Discussion

The Selection of the PEGs Blend as a PCM. PEG is polymer with a very simple chemical structure: HO-(CH_2-CH_2-O)$_n$-H. The blending of pasty and solid PEGs will produce a white pasty ointment that has good solubility in water, good dissolving properties, and is suitable for many active substances. Figure 1 shows the DSC melting curves of PEG600, PEG1000, and their melt blends with different mass ratios of PEG600 and PEG1000: 75:25, 50:50, and 25:75, respectively. The melting curves of the PEGs blends exhibited more than one melting peak, depending on their blend ratios. With an equal mass ratio of PEG600 and PEG1000 (curve c), the DSC melting curves of the PEGs blend displayed two clear peaks at 19.1 and 34.5 °C. Therefore, the PEGs blend with 50:50 wt% was selected as a PCM in this study.

If there is no interaction between the two components, the heat of fusion value of the blended PEGs is calculated as:[10]

$$\Delta H_{PEGs}=a\Delta H_{PEG_1}+b\Delta H_{PEG_2} \quad (1)$$

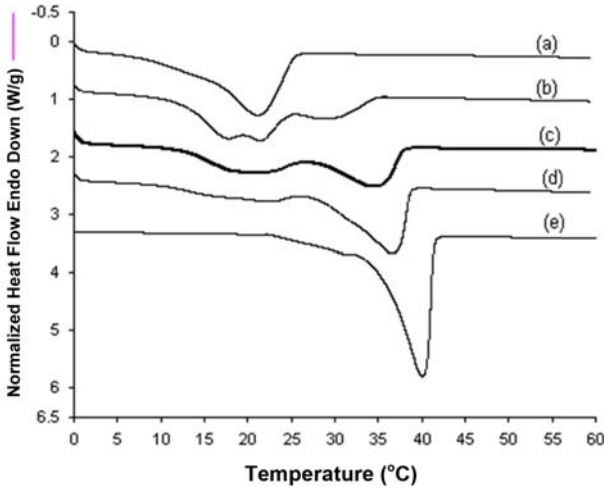

Figure 1. DSC curves of (a) PEG600, (b, c, d) PEGs blends with mass ratio of PEG600 and PEG1000; 75:25, 50:50, 25:75, (e) PEG1000.

where a and b represent the weight portion of PEG_1 and PEG_2, respectively. The values of the heat of fusion for the pure PEG600 and PEG1000 were 113.3 and 176.5 J/g, respectively. Based on the above equation, the value of the heat of fusion for the blended PEGs was 121.4 J/g, which was 15.6% lower than its theoretical value (140.4 J/g). This result implies that the synergistic effect of the co-crystallization phenomenon of PEG600 and PEG1000 might not occur as reported by Qian *et al.*[10] From Table I, it can be observed that the melting points of the blended PEG600 and PEG1000 are lower than those of the pure PEG600 and PEG1000, reducing from 21.2 to 19.1 °C and 40.1 to 34.5 °C, respectively.

Characterization of the PEGs-loaded PVDF Nanofibers.

Morphology: PVDF was used as the supporting polymer of the PCM-loaded e-spun nanofibers because of its high mechanical strength and ease of electrospinning. Figure 2 illustrates the morphology of the PVDF nanofibers and the PCM-loaded e-spun nanofibers. The average diameter of the e-spun fibers increased (from 695 to 1,541 nm) as the content of PEGs raised (from 0 to 60%) within the e-spun PVDF nanofibers. This increase in the average diameter of the e-spun PVDF nanofibers is attributed to the augmentation in the viscosity of the polymer solution due to the inclusion of viscous PEGs in the PVDF solution.[14] The higher viscosity of the polymer solution resulted in greater resistance to the stretching of the solution, hence causing the diameter of the e-spun fibers to be larger.[27]

The effect of the addition of fumed SiO_2 on the morphology of the e-spun PVDF/SiO_2 composite nanofibers was studied. As shown in Figure 3, the addition of the fumed nano SiO_2 decreased the average diameters of the e-spun PEG loaded PVDF nanofibers and it broadened the diameter distribution. It is possible that there are hydrogen bonding interactions between the hydroxyl (-OH) group in the PEGs chain and the SiO_2 network, leading to the high absorption of PEGs,[28] and therefore reducing the viscosity of the e-spun solution. In addition, the increase in the SiO_2 content did not significantly change the morphology of the nanofibers.

Thermal Properties: The thermal properties of the PEGs-loaded e-spun PVDF nanofibers were analyzed by DSC. Figure 4 shows the melting curves of the e-spun nanofibers with various percentages of PEGs. The melting curves of the form-stable PCM-loaded e-spun nanofibers demonstrated only one melting peak, indicating the overlap of the melting peaks of PEG600 and PEG1000. The data for the melting

Table I. Thermal Properties of PEGs Blends and PEGs/PVDF Composite Nanofibers with Different Ratio of PEGs Blends[a]

Sample	T_m (°C)	ΔH_m (J/g)	T_c (°C)	ΔH_c (J/g)
PEG 600	21.2	113.3	4.6	-107.2
PEG 1000	40.1	167.5	28	-124.3
PEG 1000/PEG 600 1/1 w/w	19.1/34.45	121.4	15.8	-114.8

[a] T_m=the melting temperature, ΔH_m=latent heat of melting, T_c=the crystallization temperature, ΔH_c=latent heat ofcrystallization.

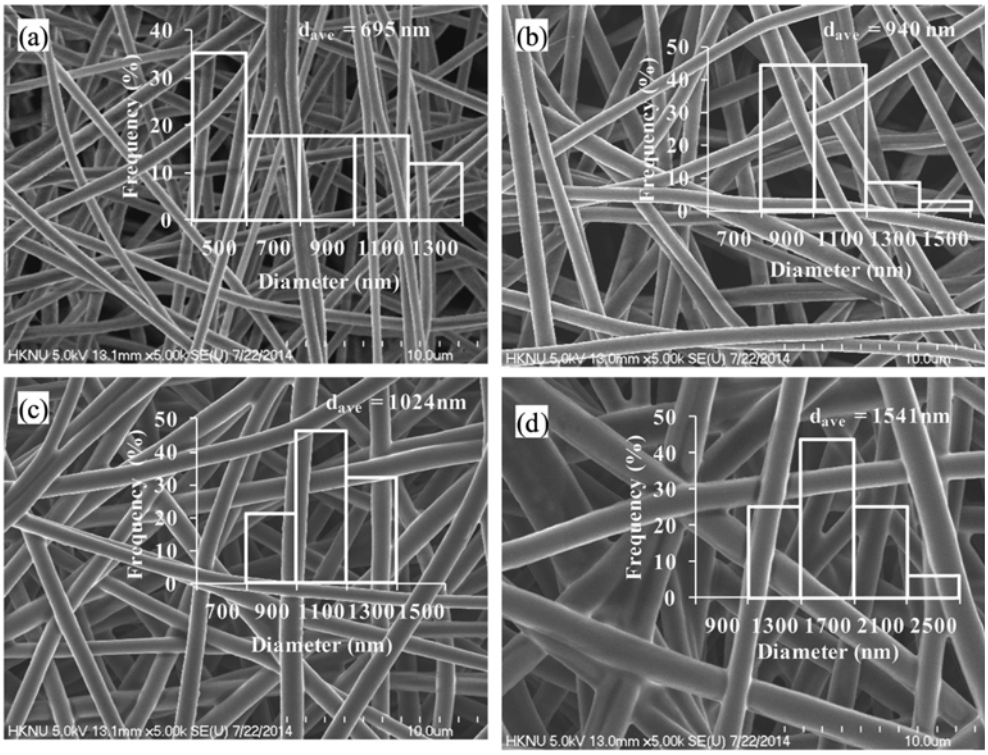

Figure 2. FE-SEM images of PCM loaded e-spun PVDF nanofibers with various percentage of PEGs blend: (a) 0% PEGs, (b) 20% PEGs, (c) 40% PEGs, and (d) 60% PEGs.

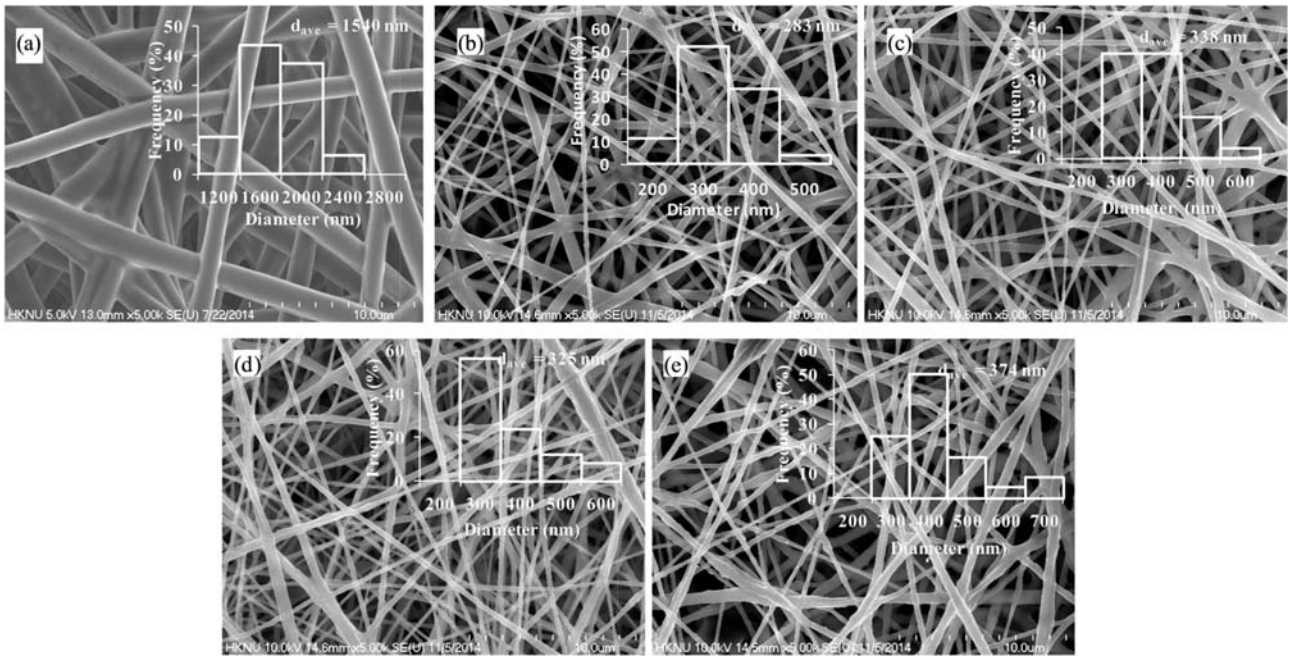

Figure 3. FE-SEM images of PCM loaded SiO_2/PVDF composite nanofibers with various percentage of SiO_2 loading: (a) 0% (b) 3% SiO_2, (c) 6% SiO_2, (d) 9% SiO_2, and (e) 12% SiO_2.

point, heat of fusion, and enthalpy ratio are summarized in Table II. The latent heat of the PEGs-loaded PVDF nanofibers increased with the augmentation of the PEGs content of the nanofibers, and hence resulting in the increase of the enthalpy ratio values. The ratio of the heat of fusion values of the PEGs-loaded e-spun PVDF nanofibers and that of the pure

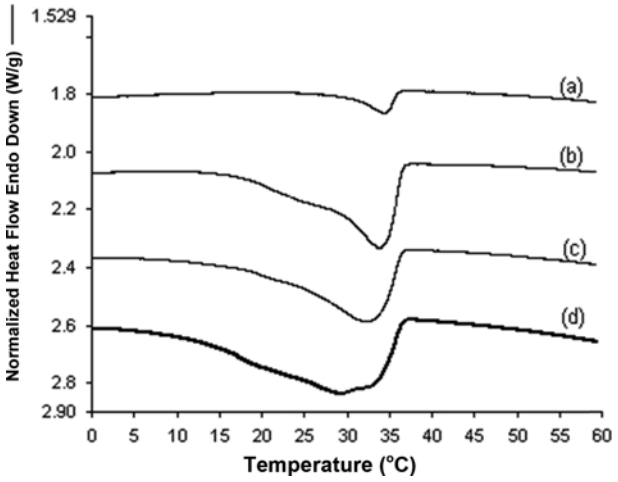

Figure 4. DSC curves of PEGs loaded e-spun PVDF nanofibers with different percentage of PEGs : (a) 20%, (b) 40%, (c) 50%, and (d) 60%.

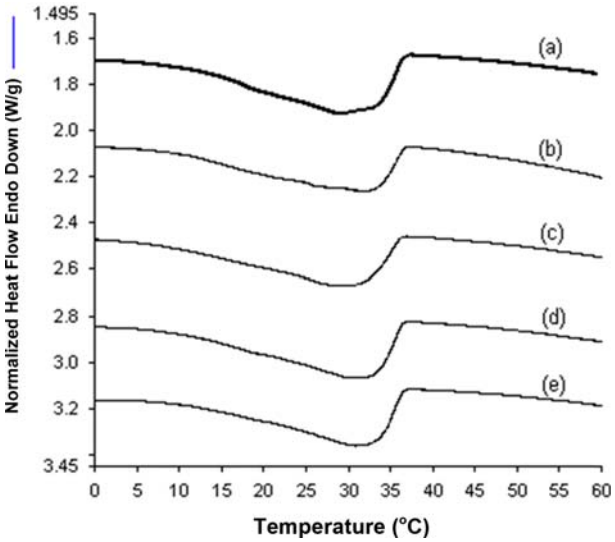

Figure 5. DSC melting curves of SiO_2/PVDF composite nanofibers with different amount of silica inclusions: (a) 0%, (b) 3%, (c) 6%, (d) 9%, and (e) 12%.

PEGs was calculated with eq. (2).[29] This ratio is a measure of the effective energy storage of the e-spun nanofibers.

$$\text{Enthalpy ratio} = \frac{\Delta H_{e-spun\ fibers}}{\Delta H_{pure\ PCM}} \times 100 \quad (2)$$

where $\Delta H_{e\text{-}spun\ fibers}$ and $\Delta H_{pure\ PCM}$ are the measured heat of fusion of the PEGs-loaded e-spun PVDF nanofibers and the PEGs blend, respectively. The highest enthalpy ratio of the PCM-loaded e-spun nanofibers was 40.3% when the PEGs content in the PEGs-loaded e-spun PVDF nanofibers was 60 wt%. The deviation in the thermal properties from their theoretical values can be explained by the lower crystalline region of the PEGs in the PEGs-loaded e-spun PVDF nanofibers. The crystallization could be hindered by the confinement effect of the PVDF matrix, which has also been reported in literature.[1,14]

The DSC melting curves of the e-spun PEGs-loaded PVDF/ SiO_2 composite nanofibers with various amounts of fumed silica are shown in Figure 5; the corresponding thermal properties are summarized in Table III. The values of T_m and ΔH_m of the PEGs-loaded PVDF/ SiO_2 composite nanofibers were similar with those of the PEGs-loaded PVDF nanofibers. This is attributed to the inertness of the fumed SiO_2 to the PVDF.

Mechanical Properties: The ultimate strength of the e-spun nanofibers was derived from tensile stress-strain curves, as shown in Figure 6. The PVDF was a supporting polymer and it provided both a form-stable structure and improved mechanical strength of the PCM-loaded PVDF nanofibers. As shown in Figure 6, both the tensile stress and elongation values of the

Table II. Thermal Properties of PEGs-Loaded PVDF e-Spun Nanofibers with Various Percentages of PCM

Sample	T_m (°C)	ΔH_m (J/g)	Enthalpy Ratio (% PEGs loading in the nanofibers)
PEG1000/PEG600 1/1 w/w	19.1/34.45	121.4	100
20% PEGs	34.4	4.3	3.5
40% PEGs	33.9	33.0	27.2
60% PEGs	29.3	48.9	40.3

Table III. Thermal Properties of PEGs-Loaded PVDF/SiO_2 Composite Nanofibers with Various Contents of Silica

Sample	T_m (°C)	ΔH_m (J/g)	Enthalpy Ratio (% PEGs loading in the nanofibers)
0% SiO_2 PEGs-Loaded PVDF Nanofibers	29.3	48.9	40.3
3% SiO_2 PEGs-Loaded PVDF Nanofibers	31.8	41.5	34.2
6% SiO_2 PEGs-Loaded PVDF Nanofibers	29.6	43.2	35.6
9% SiO_2 PEGs-Loaded PVDF Nanofibers	30.7	46.8	38.6
12% SiO_2 PEGs-Loaded PVDF Nanofibers	31.3	48.7	40.1

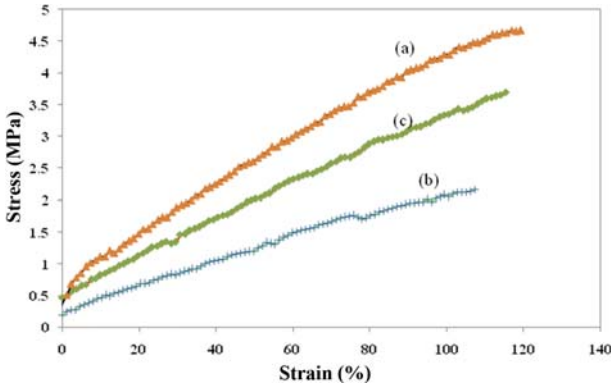

Figure 6. Tensile strength of (a) PVDF nanofibers, (b) PEGs loaded PVDF nanofibers, (c) PEGs loaded PVDF/SiO_2 composite nanofibers. Both PEGs loaded PVDF nanofibers and PEGs loaded PVDF/SiO_2 composite nanofibers contained 60 wt% of PEGs. Concentration of SiO_2 in blend of PEGs/PVDF/SiO_2 is 12 wt% (compared with the weight of PEGs).

PEGs-loaded PVDF nanofibers were lower than those of the e-spun PVDF nanofibers. This is attributed to the presence of PEGs, which had low tensile strength. Furthermore, the addition of fumed SiO_2 in the e-spun PEGs-loaded PVDF/SiO_2 composite nanofibers significantly increased the tensile strength of the composite nanofibers (from 2.17 to 3.69 MPa), and also generated a larger strain value (from 107.4% to 115.3%). The results indicate that fumed SiO_2, as inorganic filler, helped increase the mechanical strength of the e-spun PEGs-loaded PVDF/SiO_2 composite nanofibers.

Characterization of the PEGs/PVDF Core/Shell-Structured e-Spun Nanofibers.

Morphology: Figure 7(a)-(e) represents the FE-SEM images of PEGs/PVDF core/shell e-spun nanofibers with different core feed rates. With the raise of core feed rate from 1.0 to 4.0 μL/min, the average diameters of the coaxially e-spun nanofibers increased, which is similar to that of PEGs/PVDF fibers by single electrospinning. The effect of the core feed rate on the structure of core/shell PEGs/PVDF e-spun fibers was observed in Figure 8(a)-(d). It could be seen that the core/shell structure could obtained and PEGs is encapsulated completely by PVDF sheath in each fiber during the coaxial electrospinning process. Both the diameter of the core and outer layer of the shell are increased with the increasing of core feed rates. When the core feed rate was 4.0 μL/min the core/shell structure were broken down.

Confirmation of the Core/Shell Structure: The configuration of the core/shell-structured coaxial nanofibers was initially identified *via* water contact angle (WCA) measurement, by specifically checking the leakage of the hydrophilic PEGs core layer to the hydrophobic shell layer of the e-spun nanofibers. Figure 9 demonstrates the WCA of the non-woven mats of both the e-spun PVDF nanofibers and the core/shell-structured nanofibers, fabricated by coaxial electrospinning with various core feed rates. The WCA value of the non-woven mat of the e-spun PVDF nanofibers was 133.1°, indicating that the e-spun PVDF nanofibers are very hydrophobic. The WCA values for the non-woven mats of the PEGs-loaded e-spun PVDF nanofibers at core feed rates of 1.0, 2.0, and 3.0 μL/min, were 120.2°, 121.0°, and 100.5°, respectively. The WCA values of

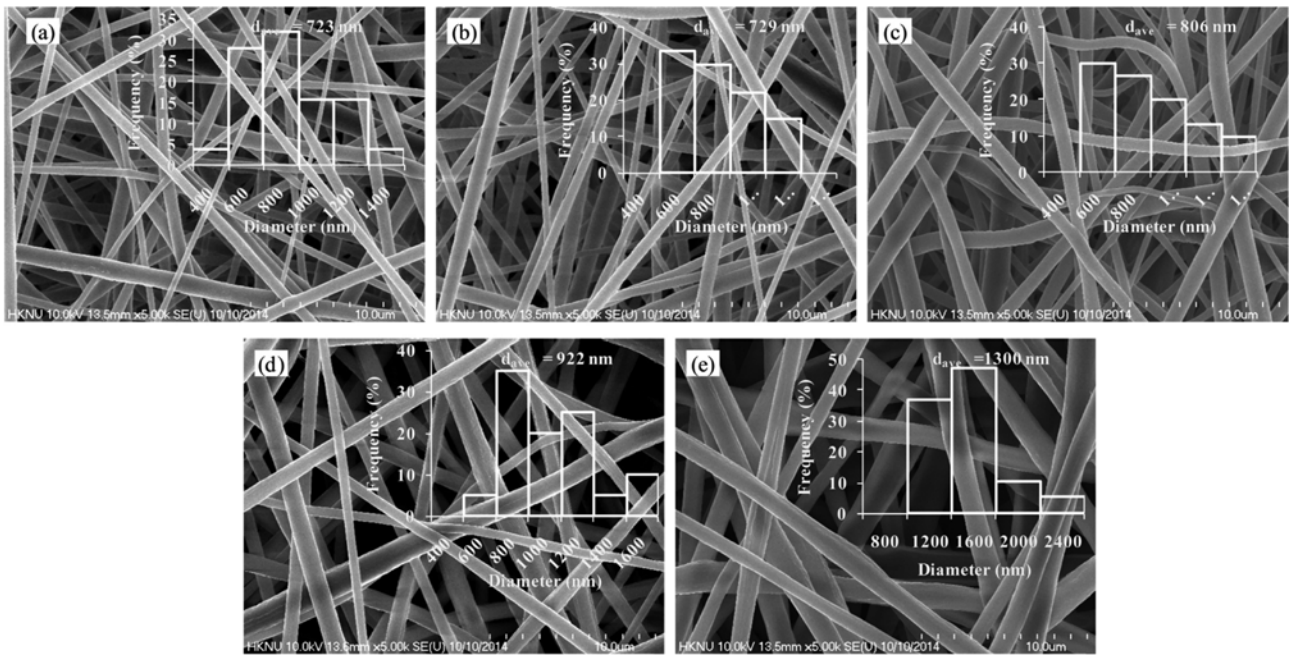

Figure 7. FE-SEM images of (a) PVDF nanofibers, (b, c, d, e) core/shell structured nanofibers, fabricated by coaxial electrospinning, with different core feed rate of 1.0, 2.0, 3.0, and 4.0 μL/min, respectively.

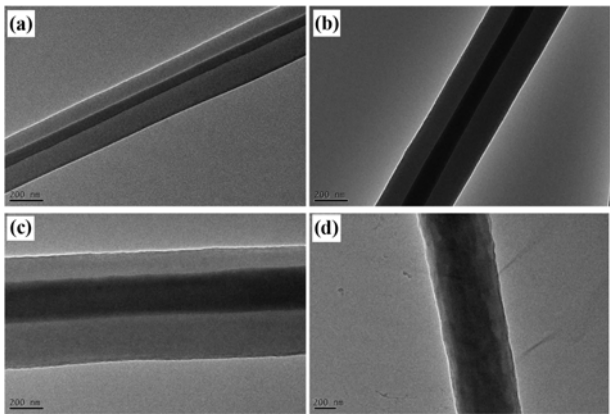

Figure 8. TEM images of e-spun PEGs/PVDF composite nanofibers fabricated by coaxial electrospinning with different core feed rate of (a) 1.0, (b) 2.0, (c) 3.0, and (d) 4.0 μL/min.

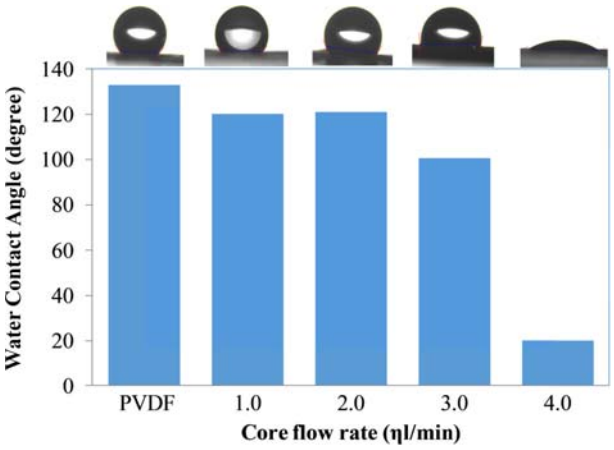

Figure 9. Water contact angles of (a) PVDF nanofibers and (b, c, d, e) core/shell structured nanofibers with different core feed rates.

the non-woven mats of the core/shell nanofibers were similar to those of the non-woven mat of the e-spun PVDF nanofibers. These results confirm that, at these core feed rates, most nanofibers were constructed of core/shell-structured nanofibers. When the core feed rate increased to 4.0 μL/min, the WCA value significantly reduced to 20.1°, indicating the leakage of PEGs on the surface of the e-spun nanofibers. This indicates that during the coaxial electrospinning, the formation of the core/shell-structured e-spun nanofibers may be hindered if the core feed rate of the PEGs is too high.

ATR-FTIR analysis was also used to confirm the core/shell structure of the fabricated nanofibers. Figure 10 demonstrates the ATR-FTIR spectra of the PEGs, PVDF, and the PEGs/PVDF core/shell nanofiber mats, fabricated at various core feed rates. The ATR-FTIR spectra of the PEGs and the non-woven mat of the PEGs/PVDF core/shell e-spun nanofibers, fabricated at core flow rates of 1.0, 2.0, and 3.0 μL/min, were quite similar. When the core feed rate attained 4.0 μL/min, the ATR-FITR spectrum of the non-woven mat of the PEGs/PVDF core/shell e-spun nanofibers exhibited two new peaks at 1093 and 2868 cm^{-1}, corresponding to C-O stretching and C-H stretching vibrations, respectively. This indicates the presence of PEGs on the outer surface of the e-spun nanofibers at a core feed rate of 4.0 μL/min.

Thermal Properties: The DSC thermograms and the corresponding data for the thermal properties of the PEGs/PVDF core/shell nanofibers at various core feed rates are shown in Figure 11 and Table IV, respectively. It can be shown from Table IV that, as the core feed rate increased, the melting temperatures of the core/shell e-spun nanofibers did not significantly change, while their enthalpy ratios increased. The amounts of PEGs loaded into the e-spun nanofibers, were calculated from the enthalpy ratio by eq. (2). The enthalpy ratio

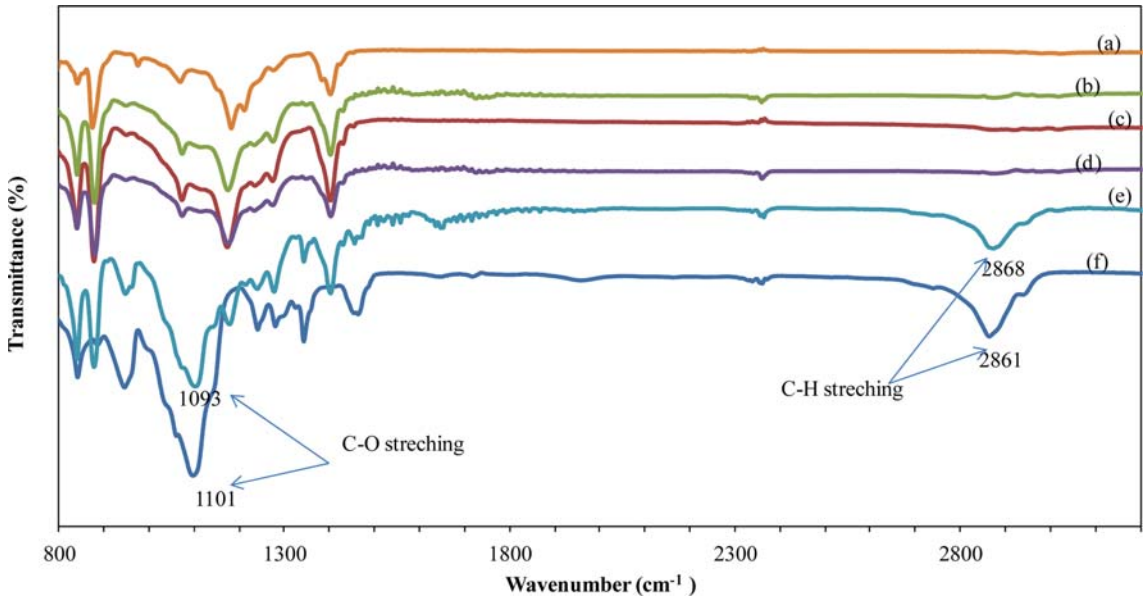

Figure 10. ATR-FTIR spectra of (a) PVDF nanofibers, (b, c, d, e) core/shell (PEGs/PVDF) structured nanofibers with different core feed rate: 1.0, 2.0, 3.0, and 4.0 μL/min, and (f) PEGs.

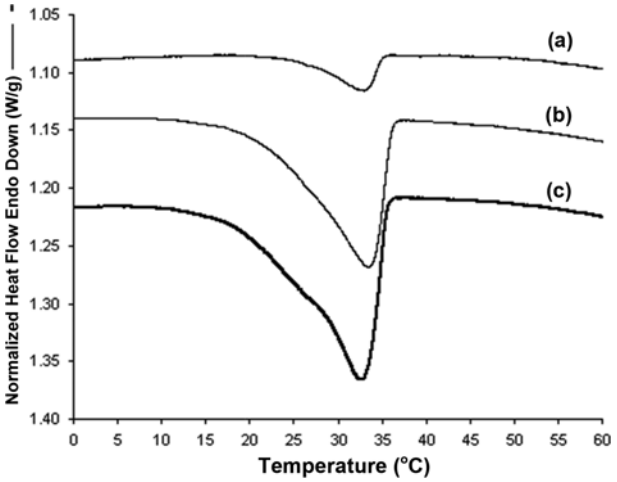

Figure 11. DSC curves of electrospun fibers of PEGs/PVDF structure at sheath flow rate of 2 mL/h and different core flow rates: (a) 1.0, (b) 2.0, and (c) 3.0 μL/min.

Table IV. Thermal Properties of the Core/Shell (PEGs/PVDF)-Structured e-Spun Nanofibers with Various Core Feed Rates

Core Feed Rates (μl/min)	T_m (°C)	ΔH_m (J/g)	Enthalpy Ratio (% PEGs loading in the fibers)
1.0	33.4	8.56	7.1
2.0	32.7	14.78	12.2
3.0	32.8	16.57	13.7

of the core/shell-structured e-spun nanofibers, fabricated at core feed rates of 1.0, 2.0, and 3.0 μL/min, were 7.1, 12.2, and 13.7 wt%, respectively. These values are much lower than those of the PEGs-loaded PVDF e-spun nanofibers, which attained 40.3% at the highest loading of PEGs by single electrospinning.

Thermal and Form-Stability Test: The form-stability of the e-spun nanofibers was examined by a DSC heating/cooling cycle test, a hot oven test, and a water immersion test.

The results of the DSC heating/cooling cycle test of the e-spun nanofibers after 1, 50, and 100 thermal cycles are displayed in Figure 12. The corresponding data is summarized in Table V. There were slight differences in the temperatures and latent heats of the phase change between the first and the 50th melting/solidification cycles. However, no deviation of the melting temperature and latent heat of the e-spun nanofibers were observed following the 50th cycle. This implies the good thermal stability of the PEGs-loaded e-spun nanofibers following long term thermal testing. After the first few cycles, the DSC melting curves of the PEGs-loaded PVDF nanofibers displayed two clear peaks. These correspond to the melting peak of PEG 600 at 20 °C and the melting peak of the PEG1000 at approximately 33 °C. The curve of the PEGs/PVDF core/shell nanofibers exhibits only one melting peak at 32.7 °C.

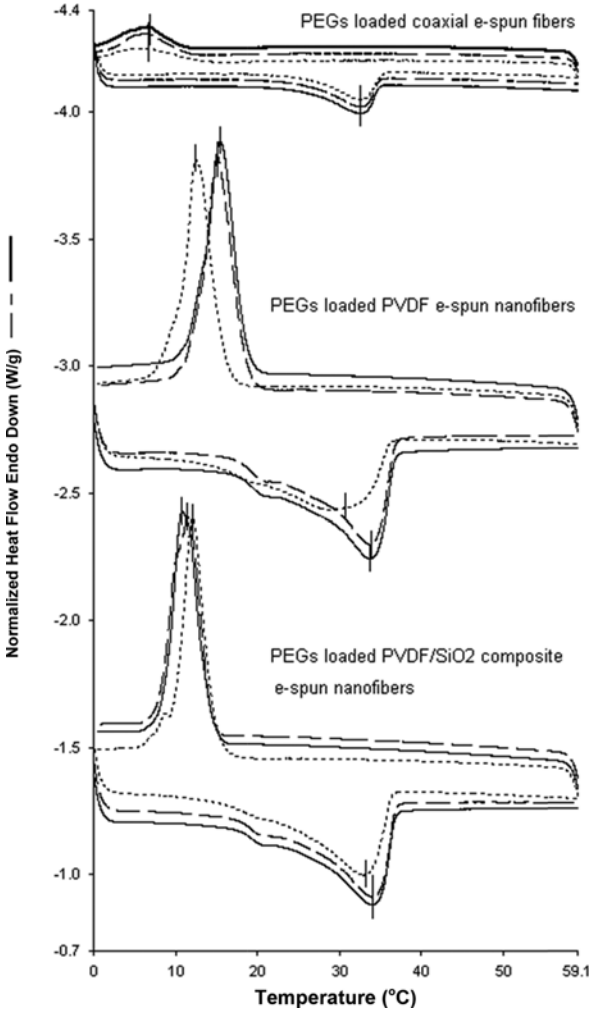

Figure 12. DSC heating/cooling curves of e-spun nanofibers after the first, 50 and 100 cycles. ·····: The first cycle, -----: After 50 cycles, ——: After 100 cycles

Table V. DSC Heating/Cooling Cycle Test

Sample		T_m (°C)	ΔH_m (J/g)
PEGs-Loaded PVDF Nanofibers	1 cycle	29.3	48.9
	50 cycles	19.8/33.7	51.1
	100 cycles	20.0/33.8	51.1
PEGs-Loaded PVDF/SiO_2 Composite Nanofibers	1 cycle	31.3	48.7
	50 cycles	19.8/33.0	50.5
	100 cycles	20.1/33.1	50.4
PEGs-Loaded Core/Shell-Structured Nanofibers	1 cycle	32.8	16.6
	50 cycles	32.6	16.6
	100 cycles	32.7	16.7

The small peak at 20 °C (observed in the melting curves of the PEGs-loaded PVDF nanofibers and the PVDF/SiO_2 com-

posite nanofibers), after many heating/cooling cycles could be partly attributed to the low level of leakage of the PEG600 from the PEGs loaded nanofibers. The melting curve of the PEGs loaded core/shell nanofibers did not show any peak at 20 ºC, indicating that there was no leakage of the PCM from the core/shell-structured nanofibers. This demonstrates the higher thermo-stability of the core/shell-structured nanofibers in comparison to the PEGs-loaded PVDF nanofibers.

The thermal and form-stability testing of the e-spun nanofibers was conducted under high temperature conditions. Figure 13 shows the SEM images of the PEGs-loaded PVDF nanofibers, the PVDF/SiO_2 composite nanofibers, and the PEGs/PVDF core/shell nanofibers, before and after heat treatments at 80 ºC for 24 h. It can be observed from Figure 13(a2) that, following heating, the average diameter of the PEGs-loaded PVDF nanofibers increased (more than 2 times), from 940 to 2,185 nm. Greater changes in the morphology were observed by maintaining the PEGs-loaded nanofibers at a higher tem-

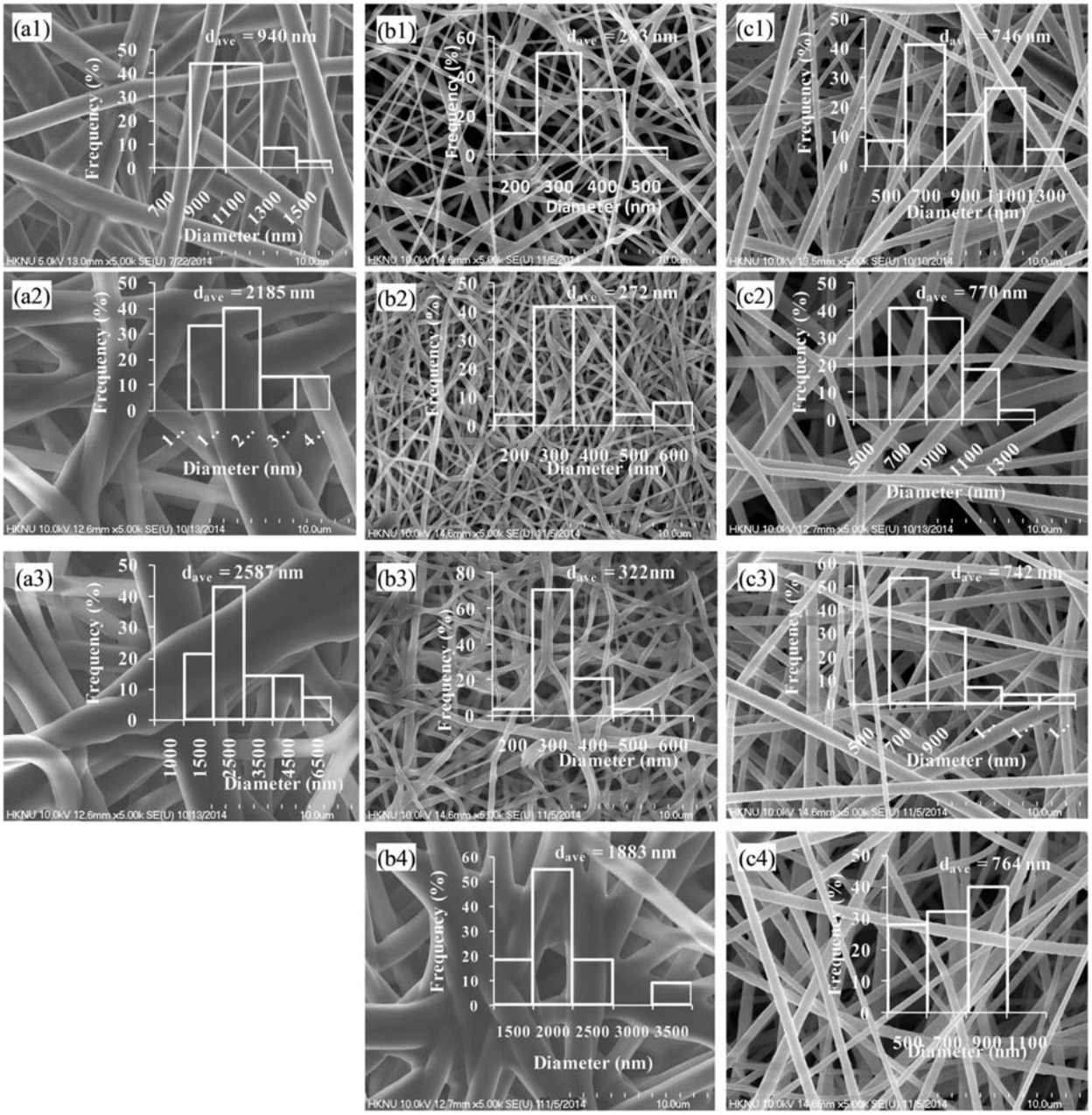

Figure 13. FE-SEM images of e-spun fibers of (a) PEGs-loaded PVDF, (b) PEGs-loaded PVDF/SiO_2 composite, and (c) PEGs-loaded PVDF core/shell fibers. The indexes 1,2,3,4 express the conditions before and after heat treatment by 24 h at 80, 120, and 150 ºC, respectively.

perature (150 ºC). This indicates the leakage of PEGs from the PVDF matrix. This phenomenon was also observed following the heat treatment of the PEGs-loaded PVDF/SiO_2 composite nanofibers. However, its average diameter increased much less than that of the PEGs loaded PVDF nanofibers. The thermal stability of the PVDF/SiO_2 composite nanofibers was more superior than that of the PEGs-loaded PVDF nanofibers, as a result of the absorption of melted PEGs by the fumed SiO_2 within the PVDF matrix. The PEGs/PVDF core/shell nanofibers (with and without heat treatments) had quite similar average diameters before and after heating, indicating that there was no leakage of PEGs from the e-spun nanofibers, and that they exist as form-stable nanofibers.

Since PEGs is a highly hydrophilic material, the PEGs could be removed from the PVDF e-spun nanofibers after the immersion of the e-spun nanofibers in water. Figure 14 shows the morphology of the e-spun nanofibers of the PEGs-loaded PVDF/SiO_2 composite nanofibers and the PEGs/PVDF core/shell nanofibers, before and after the water immersion test at 50 ºC for 12 h. The morphology of the e-spun PVDF/SiO_2 composite nanofibers changed from smooth to rough surface containing grooves and wrinkles. This was due to the dissolution of PEGs on the surface of the nanofibers immersed in water. The same test was conducted with the PEGs/PVDF core/shell nanofibers at 50 ºC for 12 h. It was observed that there were no significant changes on the surface of e-spun nanofibers before and after the water immersion test, as shown in Figure 14(b1) and (b2). The PEGs in the core were completely protected by the PVDF shell layer in the core/shell-structured e-spun nanofibers. This indicates the good form-stability of the PEGs/PVDF core/shell nanofibers fabricated by the coaxial electrospinning.

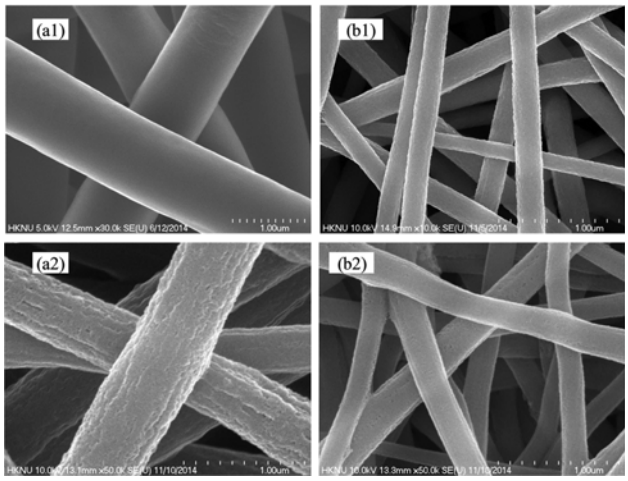

Figure 14. FE-SEM images of e-spun fibers of (a1, a2) PEGs-loaded PVDF/SiO_2 composite nanofibers and (b1, b2) PEGs-loaded PVDF core/shell structured nanofibers before (1) and after (2) water treatment. The samples were immersed in water under stirring at 50 ºC in 12 h.

Conclusions

The form-stable PEGs-loaded PVDF nanofibers were successfully fabricated by single and coaxial electrospinning. The melting point and highest enthalpy ratio of the PEGs-loaded PVDF/SiO_2 composite nanofibers were approximately 31 ºC and 40%, respectively. While the respective values for the PEGs/PVDF core/shell structure nanofibers were 33 ºC and 13.7%. With the addition of fumed SiO_2 into the PEGs/PVDF composite, the PEGs-loaded PVDF/SiO_2 composite nanofibers had greater thermal stability and mechanical strength than the PEGs-loaded PVDF nanofibers. Both the PEGs-loaded PVDF/SiO_2 composite nanofibers and the PEGs/PVDF core/shell nanofibers demonstrated thermal stability throughout 100 heating/cooling cycles via DSC. By comparison, the core/shell PEGs/PVDF nanofibers, fabricated at core feed rates of 1.0, 2.0, and 3.0 μL/min, were the most form-stable nanofibers in terms of their shape maintenance and their ability to prevent PEGs leakage after hot oven tests and water immersion tests. This study demonstrates that the non-woven mats of the PEGs/PVDF core/shell nanofibers can be used in extensive applications for thermal energy storage and fabrication of smart textile.

Acknowledgment. This research was supported by Basic Science Research Program through the National Research Foundation of Korea (No. 2014024375).

References

(1) C. Chen, L. Wang, and Y. Huang, *Polymer*, **48**, 5202 (2007).
(2) C. Chen, Y. Zhao, and W. Liu, *Renew. Energy*, **60**, 222 (2013).
(3) A. Sharma, V. V. Tyagi, C. R. Chen, and D. Buddhi, *Renew. Sust. Energ Rev*, **13**, 318 (2009).
(4) M. M. Farid, A. M. Khudhair, S. A. Razack, and S. Al-Hallaj, *Energy Convers. Manag.*, **45**, 1597 (2004).
(5) H. Fauzi, H. S. C. Metselaar, T. M. Mahlia, M. Silakhori, and H. Mur, *Appl. Therm. Eng*., **60**, 261 (2013).
(6) M. Mehrali, T. L. Sara, M. Mehdi, and T. M. I. Mahlia, *Energy Convers. Manag.*, **88**, 206 (2014).
(7) N. Han, X. Zhan, X. Wang, and N. Wang, *Macromol. Res*., **18**, 144 (2010).
(8) A. Sarı, *Appl. Therm. Eng.*, **25**, 2100 (2005).
(9) M. Rastogi, A. Chauhan, R. Vaish, and A. Kishan, *Energy Convers. Manag.*, **89**, 260 (2015).
(10) Y. Qian, P. Wei, P. Liang, Z. Li, Y. Yan, K. Ji, and W. Deng, *Energy Convers. Manag.*, **76**, 101 (2013).
(11) K. Tashiro, K. Imanishi, M. Izuchi, M. Kobayashi, I. Itoh, M. Imai, Y. Yamaguchi, M. Ohashi, and S. S. Richard, *Macromolecules*, **28**, 8484 (1995).
(12) C. Alkan, E. Günther, S. Hiebler, and M. Himpel, *Energy Convers. Manag.*, **64**, 364 (2012).
(13) H. Ryu, S. Park, S. M. Lee, S. J. Lee, W. G. Koh, I. W. Cheong, and J. H. Kim, *Macromol. Res*., **21**, 298 (2013).
(14) T. T. T. Nguyen, J. G. Lee, and J. S. Park, *J. Appl. Polym. Sci.*, **121**, 3596 (2011).

(15) W. Hu and X. Yu, *Renew. Energy*, **62**, 454 (2014).
(16) F. Li, Y. Zhao, and Y. Song, *Nanofibers*, InTech, 2010, Chap. 22.
(17) C. Alkan, K. Kaya, and A. Sarı, *J. Polym. Environ*., **1**, 254 (2009).
(18) F.-R. Zhu, L. Zhang, J.-L. Zeng, L. Zhu, Z. Zhu, X.-Y. Zhu, R.-H. Li, Z.-L. Xiao, and Z. Cao, *J. Therm. Anal. Calorim*., **115**, 1133 (2014).
(19) J. Jeon, J.-H. Lee, J. K. Seo, S.-G. Jeong, and S. Kim, *J. Therm. Anal. Calorim*., **111**, 279 (2013).
(20) H. Li, G. Fang, and X. Liu, *J. Mater. Sci.*, **45**, 1672 (2010).
(21) Y. Cai, H. Ke, L. Lin, X. Fei, Q. Wei, L. Song, Y. Hu, and H. Fong, *Energy Convers. Manag*., **64**, 245 (2012).
(22) C. Chen, L. Wang, and Y. Huang, *Chem. Eng. J*., **150**, 269 (2009).
(23) C. Chen, L. Wang, and Y. Huang, *Mater. Lett*., **62**, 3515 (2008).
(24) D. H. Reneker and I. Chun, *Nanotechnology*, **7**, 216 (1996).
(25) T. T. T. Nguyen, J. G. Lee, and J. S. Park, *Macromol. Res*., **19**, 370 (2011).
(26) S. Ali, Z. Khatri, K. W. Oh, I.-S. Kim, and S. H. Kim, *Macromol. Res*., **22**, 562 (2014).
(27) S. Ramakrishna, K. Fujihara, W.-E. Teo, T.-C. Lim, and Z. Ma, *An Introduction to Electrospinning and Nanofibers*, World Scientific Publishing, Singapore, 2005.
(28) Y. Cai, H. Ke, J. Dong, Q. Wei, J. Lin, L. Song, Y. Zhao, W. Hu, F. Huang, W. Gao, and H. Fong, *Appl. Energy*, **88**, 2106 (2011).
(29) A. Sarı, C. Alkan, A. Karaipekli, and O. Uzun, *Sol. Energy*, **83**, 1757 (2009).